

Ozone Production in the Reaction of T₂ and O₂ Gas: A Comparison of Experimental Results and Model Predictions

R. A. Failor,^{*,†} P. C. Souers,[†] F. Magnotta,[‡]

Lawrence Livermore National Laboratory, Livermore, California 94551

and S. G. Prussin[§]

Department of Nuclear Engineering, University of California, Berkeley, California 94720

(Received: October 17, 1991)

Ozone, predicted to be an important intermediate species in T₂ oxidation, was monitored in situ by UV absorption spectroscopy for 0.01–1.0 mol % T₂ in O₂ (1 atm, 298 K). These are the first measurements of a tritium oxidation reaction intermediate. The experimental results were compared with the predictions of our comprehensive model of tritium oxidation. The experimentally determined temporal variation in ozone concentration is qualitatively reproduced by the model. As predicted, the measured initial rate of ozone production varied linearly with the initial T₂ concentration ([T₂]₀), but with a value one-third of that predicted. The steady-state ozone concentration ([O₃]_{SS}) was predicted to be dependent on [T₂]₀^{0.3}, but measured values showed a [T₂]₀^{0.6} dependence, resulting in [O₃]_{SS} a factor of 4 larger than predicted for a 1.0% T₂–O₂ mixture. Addition of H₂ to the T₂–O₂ mixture, to differentiate between the radiolytic and chemical behavior of the tritium, produced a decrease in [O₃]_{SS} which was larger than predicted. Changing the reaction cell surface-to-volume ratio showed indications of minor surface removal of ozone. No reasonable variation in model input parameters brought both the predicted initial ozone production rates and steady-state concentrations of ozone into agreement with the experimental results. Though qualitative agreement was achieved, further studies, with emphasis on surface effects, are necessary to explain quantitative differences and gain a greater understanding of the oxidation mechanism.

Introduction

The rate of oxidation of molecular tritium (HT or T₂) to tritiated water (HTO or T₂O) is of great concern for the safe operation of tritium handling and nuclear fusion facilities. Two of the main reasons for concern are the factor of 25 000 increase in biotoxicity of tritiated water, as compared with molecular tritium, and the difference in chemical behavior of the two forms in tritium containment and removal systems. To date, the mechanism of the tritium oxidation reaction at room temperature and pressure is not well understood.

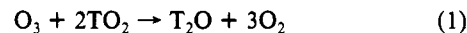
Experimental measurements of the formation rate of tritiated water have been carried out for over 30 years. The results have been fragmentary and inconsistent,^{1–8} partly due to considerable difficulty in determining tritiated water at very low concentrations. Hence, good time-dependent data for the production of tritiated water are not available.

The methods used for tritiated water detection have generally been invasive techniques, where the condensable gas was collected and analyzed for tritium using liquid scintillation counting. No in situ measurements have been made, except at very high tritium concentrations where the pressure change due to oxidation was measured.¹ Infrared absorption spectroscopy has not been used due to the low sensitivity for tritiated water. The calculated infrared band intensities of Wilemski⁹ indicate that a path length greater than 400 cm would be needed to detect approximately 2250 ppm tritiated water at 1 atm. FT-IR has not been applied to these studies and was not available for this investigation.

Chemical modeling was used to provide insight into the tritium oxidation mechanism. In two previous papers,^{10,11} we presented a comprehensive, time-dependent computer model for the homogeneous gas-phase reactions of small amounts of tritium in oxygen at 298 K and with a total pressure of 1 atm. The model included a detailed consideration of the β-radiolysis of the major species, T₂, O₂, and T₂O, and subsequent reactions of radiolysis products (ions and excited- and ground-state atoms) and major intermediate species, O₃, OT, TO₂, and, T₂O₂. The detailed mechanism for tritium oxidation predicted by our modeling in-

dicates that previous mechanisms¹² have greatly underestimated the complexity of the system.

This model predicts that the dominant overall reaction for tritiated water formation is



The predicted range of ozone concentrations should be detectable by ultraviolet absorption spectroscopy for a wide range of T₂ concentrations, even at early reaction times, and thus ozone monitoring was chosen as a sensitive test of the predicted mechanism. Though the hydroperoxyl radical, TO₂, is also of great interest, the predicted concentrations were too small to overcome the interference from UV absorption by oxygen.

In this paper, we present the results of monitoring ozone in T₂ and O₂ mixtures ranging from 0.01 to 1.1 mol % T₂ ([T₂]₀) and we compare the experimental results with the model predictions. In a number of experiments, H₂ was added to differentiate between

(1) Dorfman, L. M.; Hemmer, B. A. *J. Chem. Phys.* **1954**, *22*, 1555.

(2) Casaletto, G. J.; Gevantman, L. H.; Nash, J. B. *The Self-Radiation Oxidation of Tritium in Oxygen and Air*; Report NRDL-TR-565, U.S. Naval Radiological Defense Laboratory: San Francisco, 1962.

(3) Yang, J. Y.; Gevantman, L. H. *J. Phys. Chem.* **1964**, *68*, 3115.

(4) Eakins, J. D.; Hutchinson, W. P. *The Radiological Hazard from the Conversion of Tritium to Tritiated Water in Air by Metal Catalysis*. In *Tritium*; Moghissi, A. A., Carter, M. W., Eds.; Messenger Graphics: Phoenix, AZ, 1971; pp 392–399.

(5) Belovodskii, L. F.; Gaevoi, V. K.; Grishmanovskii, V. I.; Nefedov, N. N. *Sov. At. Energy (Engl. Transl.)* **1975**, *38*, 488.

(6) Phillips, J. E.; Easterly, C. E. *Tritium Oxidation and Exchange: Preliminary Studies*; Report ORNL/TM-5963, Oak Ridge National Laboratory: Oak Ridge, TN, 1978.

(7) Robins, J. R.; Bartoszek, F. E.; Woodall, K. B. *Review of Tritium Conversion Reactions*; Canadian Fusion Fuels Technology Project Report No. F84027; Ontario Hydro: Mississauga, Ontario, Canada, 1984.

(8) Failor, R. A.; Souers, P. C.; Prussin, S. G. *Fusion Technol.* **1988**, *14*, 1136.

(9) Wilemski, G. *J. Quant. Spectrosc. Radiat. Transfer* **1978**, *20*, 291.

(10) Failor, R. A.; Souers, P. C.; Prussin, S. G. *J. Phys. Chem.* **1986**, *90*, 5974.

(11) Failor, R. A.; Souers, P. C.; Prussin, S. G. *J. Phys. Chem.* **1988**, *92*, 429.

(12) Papagiannakopoulos, P. J.; Easterly, C. E. *Int. J. Chem. Kinet.* **1982**, *14*, 77.

[†] Chemistry and Material Sciences Department.

[‡] Physics Department.

[§] Consultant to Lawrence Livermore National Laboratory.

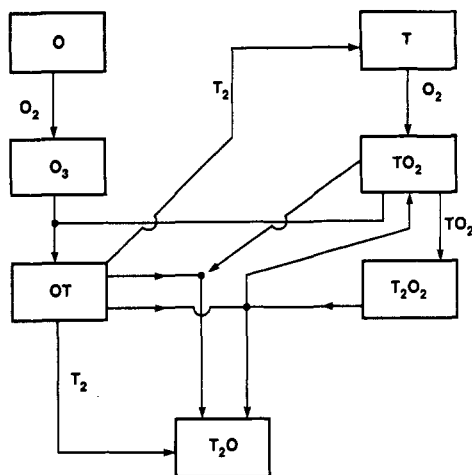


Figure 1. Schematic of main intermediates in second T₂O producing mechanism and their interaction related to the production of T₂O.

the radiological and chemical effects of the tritium on the reaction mechanism. Reaction vessels with different surface area to volume ratios were used to examine the effect of the reaction vessel surface on the ozone production.

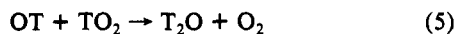
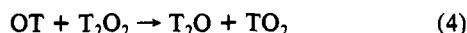
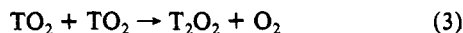
To facilitate discussion of the experimental results, this paper begins with a summary of the chemical model described in detail in ref 10 and 11, with emphasis placed on those aspects which govern the ozone concentration. Following a description of the experimental setup, the results are compared with the initial model predictions. A discussion follows of alterations to the model made in an attempt to understand why the initial model predictions are not in complete quantitative agreement with the experimental results.

Model Predictions

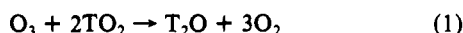
In two previous papers, we described the first detailed mechanistic model of the homogeneous gas-phase oxidation of T₂.^{10,11} The model contains over 80 reactions, including detailed radiolysis, ion-molecule and ion-electron reactions, and electronic excited-state and ground-state neutral reactions. The model's rate constants and product distributions were obtained mainly from critical evaluations of gas-phase reaction data. No attempt was made to alter the initial model input to fit any previous experimental data.

The complex model of 80 reactions can be simplified for discussion of the major reactions. During the initial reaction period, β -radiolysis of the major species induces reactions which form the major intermediate species, O, T, OT, O₃, T₂O₂, and TO₂. In ref 10, we discuss the simplification of the detailed model into the basic reactions which govern the tritiated water formation during the different time periods of the reaction.

The interactions of the main intermediate species are diagrammed in Figure 1. Oxygen and tritium atoms are produced both directly and indirectly by radiolysis. Two different reaction cycles combine the main intermediates to produce the tritiated water product:



Hence, the net production mechanism in this time period, from both cycles, is



in addition to a diminishing contribution from



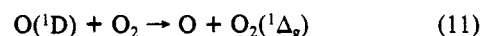
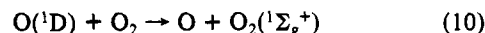
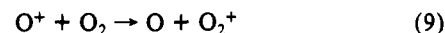
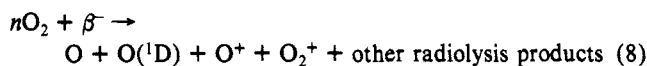
which is the dominant producer of T₂O at short times.

The production of ozone begins almost immediately after mixing the oxygen and tritium, with ozone formation controlled by the three-body reaction

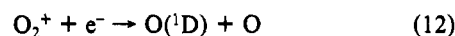


where the tertiary species, M, is predominantly O₂. Oxygen atoms are formed by a number of reactions:

(I) radiolysis induced



(II) ion-electron recombinations



and other less important routes. For all [T₂]₀, the model predicts that 60% of the total oxygen atom formation is due to the reaction of radiolysis products (eqs 8–11) and 40% from ion-electron recombination reactions (eqs 12–14).

The model calculations predict that the total oxygen atom production rate is first order in [T₂]₀. This is easy to see for eqs 8–11, which are dependent only upon the rate of radiolysis, which is dependent only on the total tritium concentration. However, it is less intuitive for the ion-electron recombination reactions, eqs 12–14.

Ozone production, through the reaction in eq 7, dominates depletion of oxygen atoms. A balance between oxygen atom production from the reactions in eqs 8–14 and ozone formation results in the oxygen atom concentration achieving steady state in less than 10⁻³ s. Since the ozone formation reaction, eq 7, is not dependent upon [T₂]₀, it is clear that dependence of the steady-state concentration of oxygen atoms, [O]_{SS}, on [T₂]₀ is first order, as is the oxygen atom formation rate. This allows us to state

$$[\text{O}]_{\text{SS}} \propto [\text{T}_2]_0 \quad (15)$$

The initial ozone production rate is a function of the steady-state oxygen atom concentration

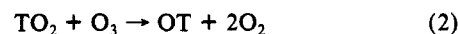
$$[d[\text{O}_3]/dt]_{\text{initial}} = k_7[\text{O}]_{\text{SS}}[\text{O}_2][\text{M}] \quad (16)$$

where k_7 is the rate constant for the ozone production reaction, eq 7. Since [M] \approx [O₂] \approx constant, eqs 15 and 16 combine to give the proportionality

$$[d[\text{O}_3]/dt]_{\text{initial}} \propto [\text{T}_2]_0 \quad (17)$$

The initial production rate of O₃ is predicted to be approximately constant for any given [T₂]₀.

Initially, there is a buildup of ozone, because no depletion reactions successfully compete with its production. As the concentrations of major intermediates increase, the ozone depletion reactions increase. The model predicts that for all [T₂]₀, ozone depletion is dominated by the reaction

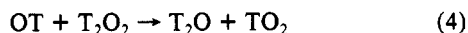
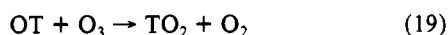


as shown in Figure 1. When the concentration of TO₂ is sufficient, this reaction controls the net rate of change of [O₃], such that ozone eventually reaches a quasi-steady state.

The initial formation of the hydroperoxyl (TO₂), like that of ozone, is dominated by a ternary reaction

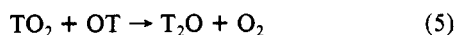
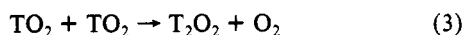


where tritium atoms, like oxygen atoms, are produced from radiolysis products and ion-electron recombination reactions. At later times, the reactions



contribute to the TO_2 formation scheme.

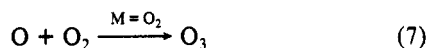
Unlike ozone depletion, no single reaction dominates the TO_2 depletion scheme for all $[T_2]_0$. The main TO_2 depletion reactions are



with the importance of each reaction varying with time. In model predictions for all $[T_2]_0$, hydroperoxyl concentration is predicted to reach steady state well before that of ozone. Therefore, we can take $[TO_2] \cong [TO_2]_{SS}$. The model also predicts that the steady-state hydroperoxyl concentration varies approximately as

$$[TO_2]_{SS} \propto [T_2]_0^{0.6} \quad (20)$$

On the basis of this analysis, two reactions dominate the ozone production and depletion



leading to

$$d[O_3]/dt = k_7[O][O_2]^2 - k_2[O_3][TO_2] \quad (21)$$

for the approximate ozone rate expression. Equation 21 can be used to determine the approximate predicted dependence of $[O_3]_{SS}$ on $[T_2]_0$. From eq 21 we then obtain

$$[O_3]_{SS} \cong \frac{k_7[O]_{SS}}{k_2[TO_2]_{SS}} \quad (22)$$

where k_7 incorporates the constant oxygen concentration into k_7 . Using the dependence of $[O]_{SS}$ and $[TO_2]_{SS}$ on $[T_2]_0$ (eqs 15 and 20), we have

$$[O_3]_{SS} \propto \frac{[T_2]_0^{1.0}}{[T_2]_0^{0.6}} \rightarrow [T_2]_0^{0.4} \quad (23)$$

Actually, calculations with the full model predict

$$[O_3]_{SS} \propto [T_2]_0^{0.3} \quad (24)$$

The model predictions regarding ozone production and steady-state concentration can be summarized by two equations, eq 24 and

$$[d[O_3]/dt]_{initial} \propto [T_2]_0 \quad (17)$$

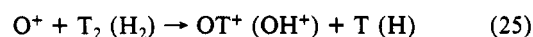
These equations were used to predict the level of ozone produced during the tritium oxidation experiments.

Effects of H_2 Addition

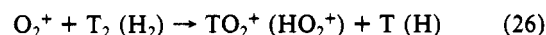
It is important to note that the chemical and radiolytic properties of tritium affect different aspects of the oxidation mechanism. The radiolytic action drives formation of the oxygen and tritium atoms, but chemical properties drive the reactivity of the T atoms, TO_2 , T_2O_2 , and other such species. To separate these effects, we have studied the effect of additions of hydrogen, H_2 , in both the model calculations and experiments. The rate constants for the hydrogen-based reactions in the model were adjusted for the kinetic isotope effect.¹⁰

The effects of H_2 addition on the model predictions are relatively complex. The principle influence on ozone concentration arises from an increased rate of removal of two main O_2 radiolysis products, O^+ and O_2^+ . The accelerated removal of O^+ by the

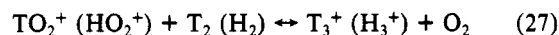
reaction in eq 25 reduces the total oxygen atom concentration, and thereby reduces ozone production (eq 16).



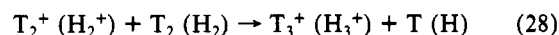
Adding H_2 removes O_2^+ by the reaction



increasing the formation of HO_2^+ . This shifts the equilibrium between $TO_2^+(HO_2^+)$ and $T_3^+(H_3^+)$ via

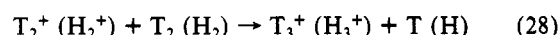
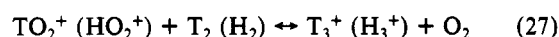
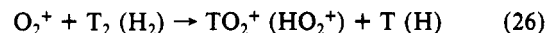


However, the buildup of HO_2^+ due to H_2 addition is countered by increased production of $H_3^+(T_3^+)$ through the reaction

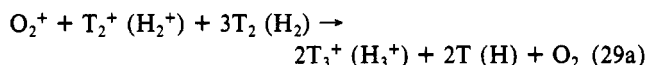


$T_2^+(H_2^+)$ is the major tritium (hydrogen) radiolysis product, and its production is therefore dependent upon the radiolytic effect of the total tritium concentration and the combined concentration of H_2 and T_2 .

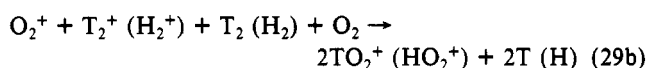
To summarize the reactions



combine, resulting in an overall reaction of either



or



depending on which direction of the equilibrium in eq 27 dominates. Whether the reaction in eq 29a or 29b dominates depends upon the rates of reactions 26–28 and the T_2/H_2 ratio.

The effects of the overall reactions shown in eq 29a,b on the steady-state ozone concentration are still not readily obvious. The model assumes that electron-ion recombination reactions decompose the ion into its constituent atoms. Therefore, H_3^+ will produce three H atoms and HO_2^+ will produce one H atom and two O atoms. If the overall reaction shown in eq 29a dominates, ozone will be diminished by reaction with TO_2 (HO_2) formed from the T (H) atoms reaction with O_2 . Eight T (H) atoms will ultimately be formed from the overall reaction in eq 29a, six from electron recombination of two $T_3^+(H_3^+)$ and two from two T (H). If the overall reaction shown in eq 29b dominates, it will not diminish ozone. This is because electron recombination of two $TO_2^+(HO_2^+)$ ions will form four oxygen atoms resulting in four ozone molecules, which will balance the TO_2 (HO_2) formed from four T (H) atoms.

Though it is a complicated system, the model predicts that at constant $[T_2]_0$ the addition of H_2 will cause a decrease in $[O_3]_{SS}$. Keeping the same H_2 concentration and increasing $[T_2]_0$ should result in an increase in $[O_3]_{SS}$. The extent of the change depends upon the H_2/T_2 ratio.

Experimental Section

The ozone concentration ($[O_3]$) was measured as a function of time by monitoring UV absorption at 253.7 nm. The hazardous quantities of T_2O which could be produced in these experiments, necessitated secondary containment around the reaction cells. To accommodate this, a double-beam spectrophotometer was constructed with both the sample and reference cell housed in a glovebox. The glovebox contained both the sample and reference reaction cells to avoid variations in length or gas composition of the optical paths (see Figure 2).

A deuterium lamp was chosen as the light source to provide a line free continuum in the ultraviolet. This allowed continuous absorbance measurements over the ozone Hartley band during each run to assure that the measured absorbance was due to ozone.

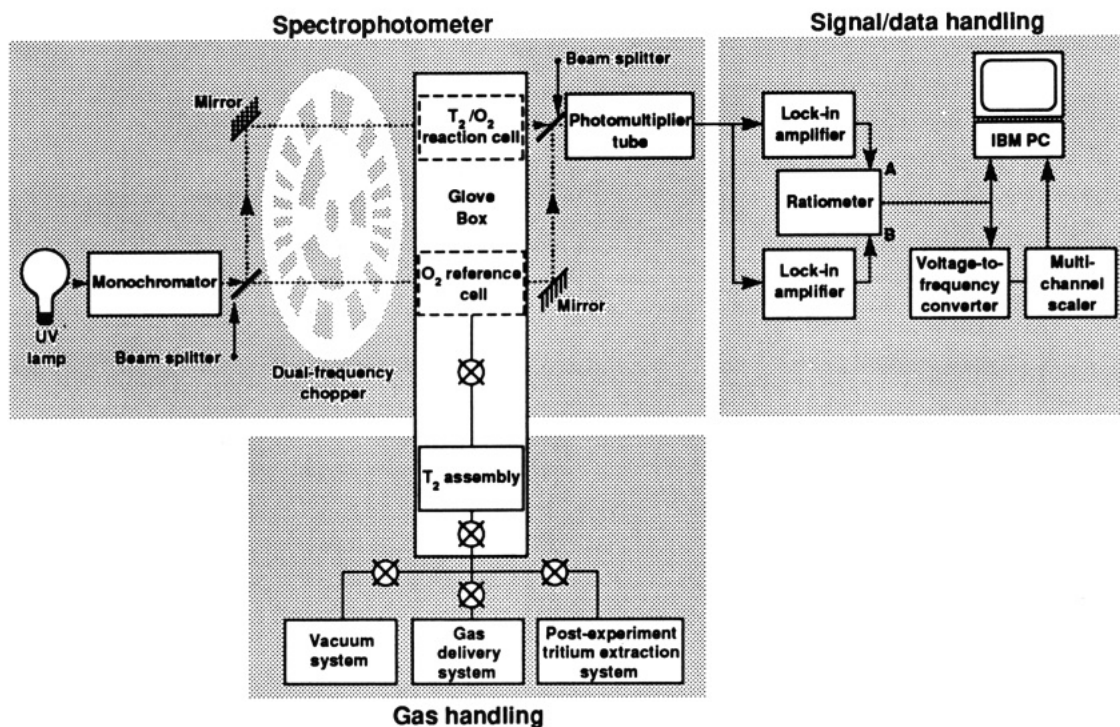


Figure 2. Schematic of experimental apparatus; spectrophotometer, gas handling system, and data acquisition.

It also permitted attempts at detecting tritiated peroxide (T₂O₂), which our modeling predicted would also be present. Ultraviolet light from the lamp was attenuated and dispersed prior to entering the two cells to eliminate the production of ozone in the beam path and the reaction vessels due to O₂ photolysis by high intensity, broad band UV light.

Exiting the monochromator, the beam passed through a UV beam splitter to provide reference and sample beams, which were chopped by a dual-cut chopping wheel, and then entered the glovebox through Spectrosil windows. The argon box atmosphere was continuously purged to avoid buildup of any possible photolysis products which would affect the relative beam intensity. The reference cell was filled to 760 Torr with oxygen and was refilled on alternate runs.

The reaction cells were made of Pyrex with sapphire end windows and a 40.0-cm long optical path. Two different diameter sample cells were used. The primary cell was 10 cm in diameter over the central 30 cm of its length. The windows were 2.5 cm in diameter and were connected to the central portion by 5-cm long sections of graded glass seal. The secondary, narrow cell was 2.5 cm in diameter over its entire length and was used in only four experiments. Each cell had three glass stopcocks at the top of the cells for gas transfer. Cell volumes were measured by PVT expansion from a precisely calibrated volume. The primary (10-cm) cell and connecting lines held a volume of 1925 ± 3 cm³ with an approximate surface area of 1000 cm². The narrow (2.5-cm) cell and connecting lines had a volume of 232 ± 3 cm³ with an approximate surface area of 320 cm². (The cell surface areas were calculated and not measured.) Prior to the first run, the cells were rinsed repeatedly with high purity water and then heated in a glass annealing oven for over 12 h. The cells' surfaces received no special chemical treatment. Just before each run, a cell was heated to over 100 °C under vacuum for more than 4 h to remove surface absorbed species, such as water.

The beam intensities were measured using an InGaAs photocathode (RCA No. C31034B) photomultiplier tube (PMT) with a UV transmitting window, operated at -20 °C and -1500 V. The PMT output signal was deconvoluted using two Stanford Research Systems (SRS) SR530 lock-in amplifiers with reference signals from the chopping wheel. The individual output voltages from the lock-in amplifiers and the ratio of the two voltages were sampled and recorded with an IBM PC-XT using the software provided by SRS.

When the signal's rate of change was negligible, a secondary method of data collection was used to obtain 2–20-s time accumulations of the sample/reference ratio. A voltage-to-frequency converter summed the ratio signal to provide input to a multi-channel scaler whose output was stored for later data analysis.

Background measurements were made with blank cells, with oxygen, and with a combination of oxygen and hydrogen. In no case was a detectable signal apparent, nor was there any change in the intensity ratio detected due to the addition of hydrogen or oxygen into the sample cell. The intensity ratio from a mixture of 2.5% H₂ in oxygen at 760 Torr in the sample cell and the reference cell at vacuum was monitored for 24 h. During that time the maximum variation in the sample/reference ratio was equivalent to less than 0.15 ppm ozone.

Prior to an experimental run, T₂ was extracted from a pure tritium-palladium storage bed filling a 50-cm³ reservoir bottle to a pressure of 1000 Torr. The T₂ purity was greater than 98% T₂ with approximately 1% DT, part per million levels of ³He and D₂, and less than 100 ppm methane. The amount of tritium needed was expanded from the reservoir bottle into a precisely calibrated volume. The background sample/reference intensity ratio was measured and checked for signal stability prior to mixing the T₂ and O₂ in the evacuated sample cell.

Oxygen (Matheson, 99.99% purity) was passed through a column of P₂O₅ to remove residual H₂O and then mixed, in the cell, with T₂, which had been expanded into the empty sample cell from the calibrated volume. The total pressure of gas in the cell was measured with a 1000-Torr MKS Baratron capacitance manometer. The pressure for individual runs was known to within 2 Torr and the average total pressure in all experiments was 760 ± 25 Torr. The temperatures of the cells and the glovebox were monitored throughout the experiment, but no attempt was made at regulation. The average temperature was 21.8 °C with temperature variation during a given experiment of ± 1.5 °C.

In experiments using H₂ and T₂, hydrogen was introduced by adding it to the T₂ already present in the calibrated volume. This mixture was then expanded into the reaction cell and then mixed with the O₂.

Absorbance measurements were continued for 20–30 h after the gases were mixed. For each run a measurement was made of the variation in sample/reference intensity ratio as a function of wavelength in the range of 230–300 nm at a time (approximately 15–20 h after mixing of the gases) when the rate of change

TABLE I: Summary of Experimental and Model Results

[T ₂] ₀ , %	[H ₂] ₀ , %	cell diam, cm	[O ₃] _{ss} , ppm		initial rate, ppm/s		1/e - time to steady state, s		expt/model steady state		
			expt	model	expt	model	expt	model	[O ₃] _{ss}	rate	time
1.09	0	10	49.5	12.5	1.1 × 10 ⁻²	2.5 × 10 ⁻²	2300	210	4.0	0.44	11.0
0.99	0	10	55.0	12.5	7.2 × 10 ⁻³	2.3 × 10 ⁻²	3350	230	4.5	0.31	14.6
0.83	0	10	35.0	11.5	5.5 × 10 ⁻³	1.9 × 10 ⁻²	2375	260	3.0	0.29	9.1
0.10	0	10	14.9	6.8	8.8 × 10 ⁻⁴	2.4 × 10 ⁻³	7350	1200	2.2	0.37	6.1
0.092	0	10	14.8		1.0 × 10 ⁻³		6800				
0.036	0	10	9.8 ^a	4.5	3.5 × 10 ⁻⁴	8.3 × 10 ⁻⁴	10550	2260	2.2	0.42	4.7
0.034	0	10	7.8		3.1 × 10 ⁻⁴		10250				
0.028	0	10	4.9	4.1	1.5 × 10 ⁻⁴	6.5 × 10 ⁻⁴	9900	3480	1.3	0.23	2.6
0.027	0	10	5.3		1.9 × 10 ⁻⁴		9000				
0.010	0	10	1.7 ^b	3.1	2.7 × 10 ⁻⁵	2.4 × 10 ⁻⁴	19750	5530	0.5	0.11	3.6
0.098	1.18	10	8.3	6.0	6.7 × 10 ⁻⁴	2.2 × 10 ⁻³	3100	1330	1.4	0.30	2.3
0.099	0.88	10	7.1	6.1	8.2 × 10 ⁻⁴	2.3 × 10 ⁻³	2750	1260	1.2	0.36	2.2
0.098	0.50	10	8.2	6.3	8.9 × 10 ⁻⁴	2.4 × 10 ⁻³	2900	1230	1.3	0.37	2.4
0.032	1.01	10	5.0	3.4	2.8 × 10 ⁻⁴	7.3 × 10 ⁻⁴	6000	2240	1.5	0.38	2.7
0.032	0.08	10	7.0	3.7	3.2 × 10 ⁻⁴	7.6 × 10 ⁻⁴	7620	2050	1.9	0.42	3.7
0.027	0.76	10	5.1	3.2	1.8 × 10 ⁻⁴	6.4 × 10 ⁻⁴	6900	2420	1.6	0.28	2.9
0.019	0.59	10	2.9 ^b	2.7	1.2 × 10 ⁻⁴	4.4 × 10 ⁻⁴	16000	2960	1.1	0.27	5.4
0.930	0	2.5	48.0	11.9	8.9 × 10 ⁻³	2.3 × 10 ⁻²	2000	240	4.0	0.39	8.3
0.100	0	2.5	9.1	6.8	8.9 × 10 ⁻⁴	2.4 × 10 ⁻³	3750	1200	1.3	0.37	3.1
0.110	0	2.5	8.8		8.9 × 10 ⁻⁴		3800				
0.030	0	2.5	3.2 ^b	4.2	1.4 × 10 ⁻⁴	7.0 × 10 ⁻⁴	8000	3450		0.20	

^aSignal problem; value probably high. ^bDid not achieve full steady state.

of ozone concentration was negligible. Following the end of the experiment, the gas was cycled several times through a molecular sieve to destroy the ozone, and the spectral variation was re-measured. The difference in the intensity ratios with and without O₃ was divided by the ozone cross section and was found to be constant for wavelengths in the range 240–290 nm, indicating that the absorbance in this region was due solely to ozone. The signal-to-noise ratio from 230 to 240 nm was too low to tell if absorbance here was purely due to O₃ or had contributions from other species, such as T₂O₂. Peroxides are also adsorbed by the molecular sieve. The signal-to-noise ratio from 290 to 300 nm was too small to obtain any useful information from this region.

The ozone cross-section value of Hearn et al. at 253.7 nm, 1.147 × 10⁻¹⁷ cm² (±1.5%)¹³ was used in our calculations. Although more recent values differ slightly from this,¹⁴ the use of the Hearn value permitted direct use of the cross sections of Paur and Bass¹⁵ (240 ≤ λ ≤ 300 nm), which are normalized at 253.7 nm to the Hearn measurement. Only minor changes (less than a percent) in the ozone concentration values would be found by use of the cross sections in ref 14.

The uncertainties in ozone concentrations were estimated from uncertainties in intensity ratio values, path lengths, cross sections, wavelength, temperature, and pressure. The minimum uncertainty is approximately ±0.2 ppm with uncertainties of ±0.6 ppm at 10 ppm O₃ and ±3 ppm at 50 ppm O₃. Uncertainties in [T₂]₀ varied from ±0.007% for 1% [T₂]₀ to ±0.00036% for 0.01% [T₂]₀. In replicate runs reproducibility of results was excellent and generally was well within the estimated experimental uncertainties.

Experimental Results and Comparison with Model Predictions

Twenty-one experimental runs were made. In every case the measured ozone concentration exhibited an initial steady rise, followed by a decreased rate, until a constant ozone concentration was obtained. Examples of the time dependence of ozone concentrations are shown in Figure 3a,b for initial tritium concentrations of approximately 1 and 0.03%. The calculated error bars are shown in this figure.

This time dependence for the ozone concentration was predicted by the model calculations. The time dependence of ozone con-

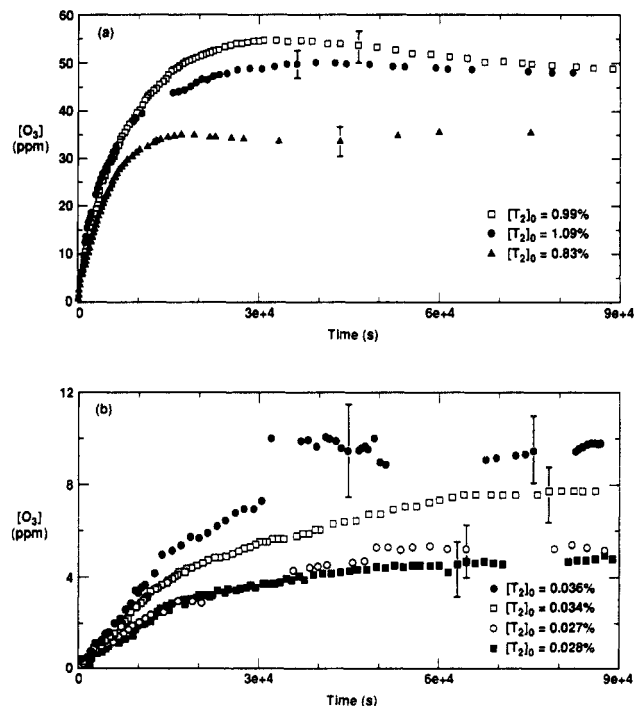


Figure 3. Concentration of ozone versus time for T₂ in O₂ (error bars are shown): (a) [T₂]₀ from 0.83 to 1.09%; (b) [T₂]₀ from 0.027 to 0.036% (outliers in the [T₂]₀ = 0.036% experiment were due to experimental difficulties).

centrations in both experiment and model predictions is well described by

$$[O_3]_t = [O_3]_{ss} [1 - \exp(-t/\tau)] \quad (30)$$

where t is time and τ is a system dependent variable.

In Table I the results from all runs are presented and compared with the associated model predictions. Included in Table I are the steady-state ozone concentration ([O₃]_{ss}), the initial rate of O₃ production, and the times (t) for [O₃] to reach 1/e of [O₃]_{ss}. The experimental initial rate was calculated by correcting early time data for the background (noise) level and then fitting the data to a linear function. In four runs, with the lowest levels of [T₂]₀, the ozone level did not fully reach a steady state. These are noted in the table.

(13) Hearn, A. G. *Proc. Phys. Soc. London* **1961**, *78*, 932.

(14) Mauersberger, K.; Barnes, J.; Hanson, D.; Morton, J. *Geophys. Res. Lett.* **1986**, *13*, 671.

(15) Paur, R. J.; Bass, A. M. *Atmospheric Ozone, Proceedings of the Quadrennial Ozone Symposium*, Halkidiki, Greece, Sept 1984; Reidel: Boston, 1985; p 611.

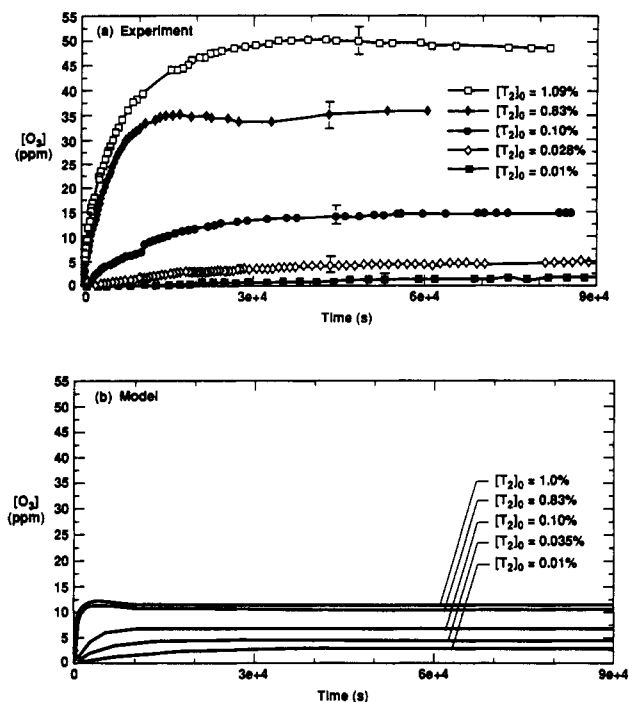


Figure 4. Concentration of ozone versus time for five concentrations of T₂ in O₂: (a) experimental results; (b) model predictions.

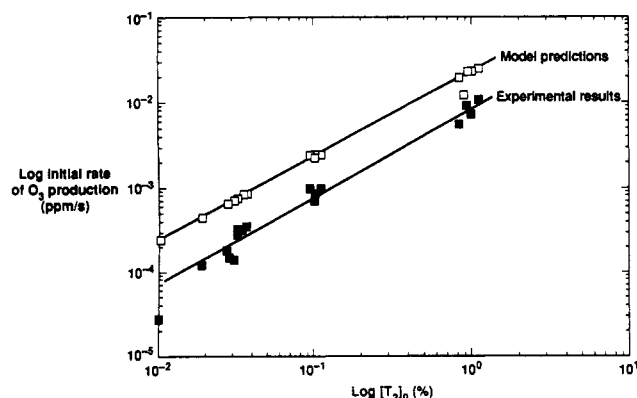


Figure 5. Initial rate of ozone production versus [T₂]₀: experimental results and model predictions.

The table is divided into three sections; the first contains results from experiments when T₂ + O₂ were reacted in the 10-cm-diameter cell, the second when T₂ + H₂ + O₂ were reacted in the 10-cm-diameter cell, and the third when T₂ + O₂ were reacted in the 2.5-cm-diameter cell. Since the model assumes homogeneous reactions only, the model calculated parameters do not reflect any surface effects whatsoever.

A. T₂ + O₂ in a 10-cm Cell. A wide range of initial T₂ concentrations, [T₂]₀, (0.01–1.09%) were studied in ten experiments. The results from five experiments, with the full range of [T₂]₀, are shown in Figure 4a, with the associated model predictions in Figure 4b. Only a fraction of the data taken are shown as data points in Figure 4a. Error bars are shown in Figure 4a. It is clear from comparing Figure 4a,b that the model provides a good qualitative prediction of experimental results but not a good quantitative agreement.

The initial rate of ozone production measured in the experiments and predicted by the model are plotted versus [T₂]₀ on the log-log plot shown in Figure 5. Since neither the addition of H₂ nor the change in cell size significantly affected the initial ozone production rate, all values from Table I have been included in the figure. The slope of the line in Figure 5 for the model predictions is 1.0 and for the experimental data is 1.1. As discussed earlier, the initial rate of ozone production is predicted to be first order in [T₂]₀

$$d[\text{O}_3]/dt|_{\text{initial}} = k_{17}[\text{T}_2]_0 \quad (17)$$

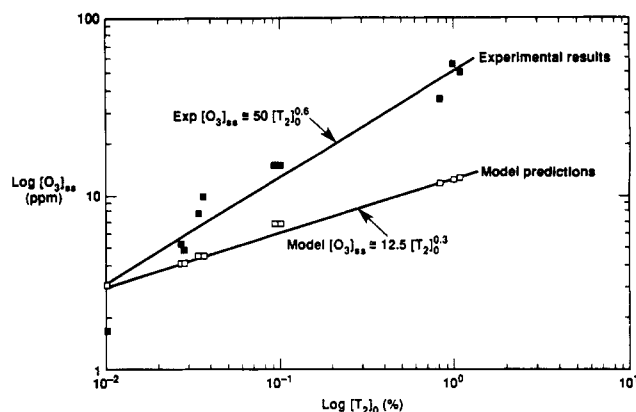


Figure 6. Steady-state ozone concentration ([O₃]_{SS}) versus [T₂]₀: experimental results and model predictions. The experimental point at 0.01% [T₂]₀ is from a run where the ozone concentration had not achieved steady state.

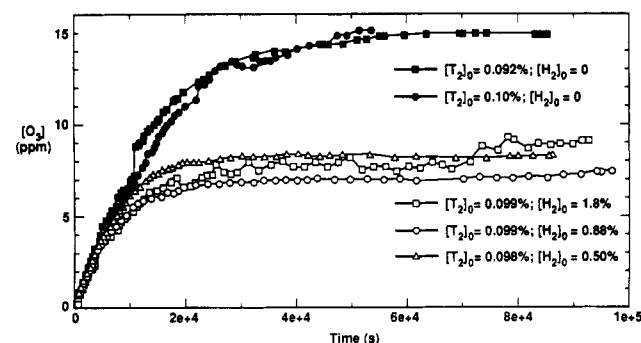


Figure 7. Experimental results for the ozone time profile for [T₂]₀ = 0.1% with and without added hydrogen.

Although this prediction seems to be in good agreement with experiment, Figure 5 shows that for all [T₂]₀ the model predicts a higher initial rate than was measured. The model-to-experiment initial rate ratio is 3.0 ± 0.7 .

The steady-state ozone concentration was found to increase with [T₂]₀. Figure 6 is a plot of the experimental and predicted [O₃]_{SS} as a function of [T₂]₀. The model prediction for the variation of [O₃]_{SS} with [T₂]₀ in T₂-O₂ mixtures is

$$[\text{O}_3]_{\text{SS}} = k_{\text{model}}[\text{T}_2]_0^{0.3} \quad (24)$$

as previously discussed. However, the measured steady-state ozone concentration varied approximately as

$$[\text{O}_3]_{\text{SS}} = k_{\text{exp}}[\text{T}_2]_0^{\sim 0.6} \quad (31)$$

In general, experimental [O₃]_{SS} values are higher than model predictions, ranging from a factor of 4 for [T₂]₀ of about 1% to less than a factor of 2 for [T₂]₀ of about 0.03%. At the lowest [T₂]₀ studied, 0.01%, the ozone concentration did not appear to achieve a true steady state, and therefore the maximum value measured is believed to be below the actual [O₃]_{SS}. It is not clear whether the experimental steady-state concentration would be greater than the predicted value in this case (see Figure 6).

B. H₂ Addition Experiments in a 10-cm Cell. To discriminate between the radiolytic and chemical effects of T₂ on ozone production, mixtures of T₂ and H₂ were added to oxygen and experiments were carried out in the same manner as described above. Three experiments were performed with [T₂]₀ at 0.1% and [H₂]₀ varying in the range of 0.50–1.18%. The results are shown in Figure 7, in addition to the results at 0.1% T₂ and no added H₂. The addition of H₂ reduced the measured [O₃]_{SS} about a factor of 2 compared with the same [T₂]₀ with no added H₂. The average value of [O₃]_{SS} in the three runs with added H₂ was 7.6 ± 0.5 ppm. Since the uncertainty estimate for the steady-state ozone concentration of individual runs was 0.4 ppm (1σ) the dependence of [O₃]_{SS} on [H₂]₀ in this range of concentrations must be quite weak. However, the presence of H₂ was responsible for the sig-

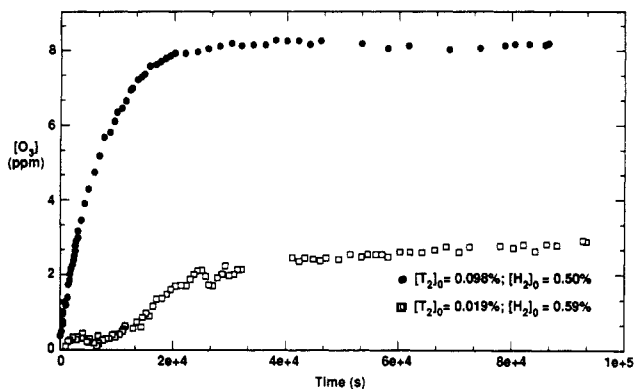


Figure 8. Experimental results for $[T_2 + H_2]_0$ of approximately 0.6% with $[T_2]_0/[H_2]_0$ at 0.03 and 0.2.

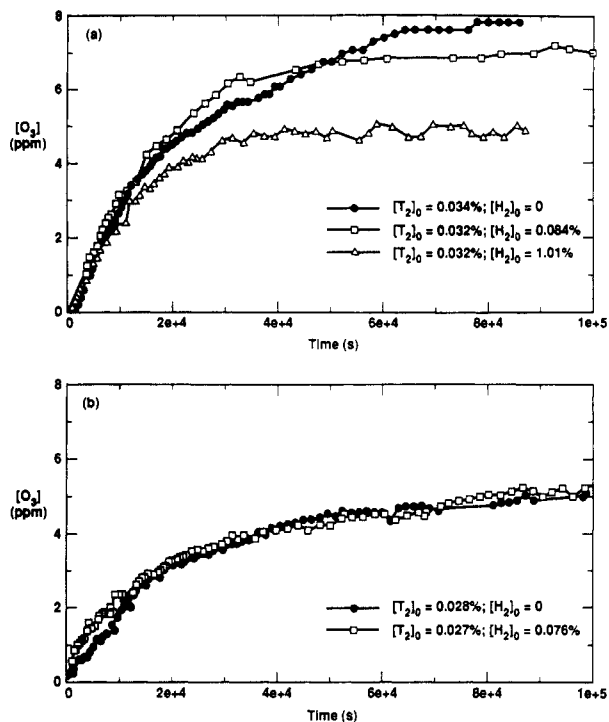


Figure 9. Experimental results for the ozone time profile for $[T_2]_0 \approx 0.03\%$ with and without added hydrogen.

nificant reduction in $[O_3]_{SS}$. For the same T_2 and H_2 mixtures as those shown in Figure 7, the model predicted a decrease of only 8–12% in $[O_3]_{SS}$ as opposed to the factor of 2 seen in the experiments. The model prediction also showed a correlation between $[H_2]_0$ and the decrease in $[O_3]_{SS}$. The model clearly underestimates the ozone depletion effects of the hydrogen species.

The model predicted that for the same total $[T_2 + H_2]$, increasing T_2 would increase $[O_3]_{SS}$. Figure 8 shows a comparison of two runs where $[T_2 + H_2]$ was approximately 0.6% but $[T_2]_0$ differed by a factor of 5 ($[T_2]_0$ of 0.098% vs 0.019%). The experiment with the greatest $[T_2]_0$ resulted in a factor of 3 larger $[O_3]_{SS}$ than was measured in the experiment with the lower $[T_2]_0$.

Data for three different T_2/H_2 ratios with $[T_2]_0$ of approximately 0.03% are shown in Figure 9. The addition of 0.08% $[H_2]$ produced only a slight decrease in the measured $[O_3]_{SS}$ compared to that with no added H_2 whereas 1.01% H_2 ($T_2/H_2 \approx 30$) caused a significant decrease in $[O_3]_{SS}$. However when 0.76% H_2 was added to 0.027% T_2 , no change was apparent in the ozone concentration. (From Figure 3b, it should be noted that the reproducibility for two runs with $[T_2]_0 = 0.027$ and 0.028% with no H_2 was excellent).

As discussed previously, the model predicts that the decrease in $[O_3]_{SS}$ is a complicated function of the $[T_2]/[T_2 + H_2]$ ratio. The experiments showed a greater decrease in $[O_3]_{SS}$ than was predicted by the model. However, understanding the detailed

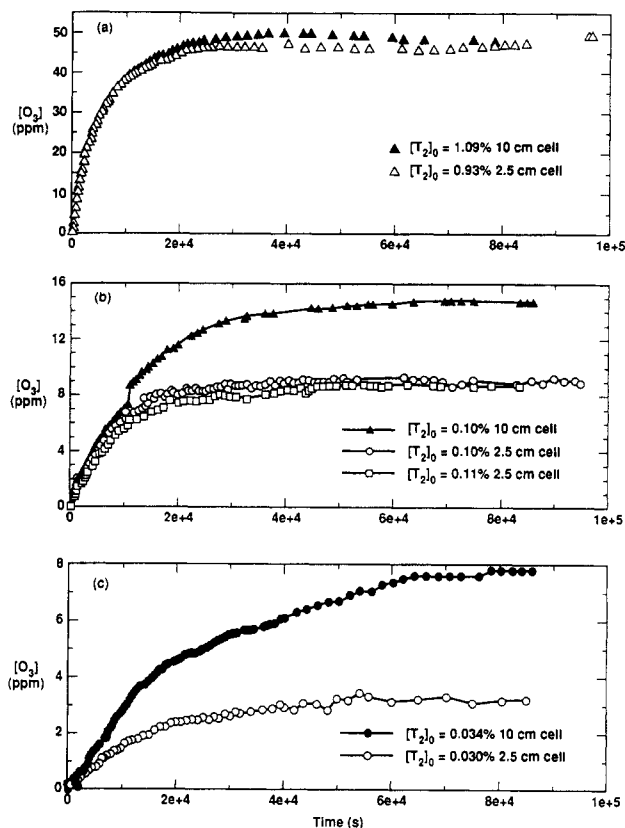


Figure 10. Surface effects: experimental $[O_3]$ versus time for 10- and 2.5-cm-diameter cells.

behavior of H_2 addition will require further study.

C. T_2 -Only Experiments in a 2.5-cm Cell. Although a complete surface-effects investigation was not attempted in our studies, some measurements were needed to evaluate the importance of reaction vessel surfaces on the ozone concentrations. As previously discussed, a 2.5-cm-diameter cell was constructed with a surface area approximately one-third that of the 10-cm-diameter cell but with a surface-to-volume ratio 2.7 times larger than that of the 10-cm-diameter cell. We expect that any surface effects would be enhanced in the 2.5-cm reaction cell.

Four experiments were run in this cell at three different T_2 concentrations (with no added H_2). Table I and Figure 10 show that the initial ozone production rate does not appear to be affected by the change in surface-to-volume ratio. This implies that the oxygen atom concentration is not greatly affected by the walls of the reaction vessel and that there is no rapid adsorption or destruction of the ozone at the walls.

At the highest $[T_2]_0$, the walls do not appear to affect the ozone concentration profile. In Figure 10a, it is clear that the 0.93% $[T_2]_0$ run in the 2.5-cm cell reproduced the data from the 1.09% $[T_2]_0$ run in the 10-cm cell. However, at lower T_2 concentrations surface effects were measurable. The results for $[T_2]_0$ of 0.1% (Figure 10b) show a reduction in $[O_3]_{SS}$ by a factor of 1.67, and for $[T_2]_0$ of 0.03% (Figure 10c) the $[O_3]_{SS}$ is reduced by a factor of 2.5, relative to $[O_3]_{SS}$ found in runs with the larger cell. The experiment was repeated at 0.1% $[T_2]_0$, and the reproducibility was excellent (Figure 10b). It appears from these results that the effect of increased surface area-to-volume ratio on $[O_3]_{SS}$ is greater for low T_2 , implying a saturation effect. This will be discussed in more detail in the next section.

Discussion

General Model Sensitivity Tests. It is evident that the model has qualitatively described the time dependence of ozone concentrations but does not quantitatively agree with experiment. To attempt to isolate the cause of the discrepancies, we first examined the general sensitivity of the model to uncertainties in the overall set of input parameters. If the experimental results were within

TABLE II: Changes Made to the Model and Their Effects on the Predicted Ozone Initial Rate and Steady-State Concentration^a

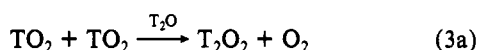
change made to model	effect on initial rate of O ₃ production	effect on [O ₃] _{SS}
Changes In Oxygen Radiolysis Rates and O Atom Reactions		
decrease O ₂ radiolysis rate	large decrease	large decrease at all [T ₂] ₀
increase O ₂ radiolysis	large increase	large increase at all [T ₂] ₀
decrease O atoms from radiolysis	small decrease	small decrease
increase O + O recombination	none	none
decrease ion + e ⁻ forming O atoms	small decrease	small decrease
ion + e ⁻ produces molecules	small decrease	small decrease
Changes in Assumptions of Oxygen-Ion Clusters		
O ₂ -ion clusters forming O atoms	large increase	large increase at all [T ₂] ₀
Changes in Hydroperoxyl System Reactions		
decrease TO ₂ + O ₃	none	large increase at all [T ₂] ₀
increase TO ₂ + TO ₂	none	large increase
decrease ion + e ⁻ to T atoms	none	small increase
ion + e ⁻ produce molecules	small decrease	small decrease
decrease T ₂ radiolysis	none	small increase
decrease T atom production	none	none
Impurity Effects		
add methane reactions	large decrease	none
react O, T atoms + impurity	small decrease	none
Addition of Electron Attachment Reactions		
O ₂ ⁻ formation added	large decrease	large decrease
Effects of Reducing Upper Limit Rate Constants		
O ₂ ⁺ + T ₂ rate reduced	small increase	small increase
Wall Adsorption of Ozone		
O ₃ adsorption on walls	none	large decrease

^aIn order for the changes to agree with the experimental results, they must produce a large decrease in the initial rate of ozone production and a large increase in [O₃]_{SS}.

the range of results predicted by a general variation of input reaction rate constants within their accepted uncertainties, then the problem would likely lie not in the model assumptions but in the input values.

We previously tested the sensitivity of the T₂O formation model predictions to input rate constants¹⁰ by allowing a random variation of all rate constants within a normal distribution covering the range of uncertainty in accepted values for the rate constants.^{16,17} These sensitivity tests were re-examined to determine if the experimental O₃ profiles were within the general uncertainties of the input data. Figure 11 shows the changes in the predicted ozone profile with these random changes for a 0.1% T₂ + O₂ mixture as compared to the original model results. The experimental data are shown for comparison.

It is evident that none of the sensitivity tests reproduces the experimental data. In one sensitivity test the random variation in the rate constants produced a change where the ozone concentration was not predicted to reach steady state. The results of this test are the uppermost curve in Figure 11. In this sensitivity test random alterations in the rate constants resulted in an overall reduction in TO₂ production and an increase in the rate constant for the reaction¹⁸



The rate constant for the reaction in eq 3a has a relatively large uncertainty, and increasing this rate within this uncertainty range, coupled with a decrease in TO₂ production, had a significant effect on the predicted ozone concentration at long times. The reduction in [TO₂] due to this coupled effect was sufficient to reduce the

ozone depletion to the point that the ozone concentration continued to increase over the time period examined. The ozone concentration did not achieve steady state. Clearly, the prediction based upon this set of input parameters does not represent a better approximation to the experiment than the unaltered model.

From these sensitivity tests, as well as others not reported here, we conclude that random variation in the input rate constants within their estimated uncertainties could effect a reduction in the initial ozone production rate by up to a factor of 2, but not the factor of 3 by which the mean value of the model predictions exceeded the experimental measurements, (see Table I). But the experimentally determined [O₃]_{SS} values were not reproduced by any of the sensitivity tests.

Specific Model Sensitivity Tests. Therefore, changes in the model seem to be needed before the model can reproduce experimental results. For this purpose, we have created altered versions of the model, not to force-fit the model to the data, but to identify the assumptions and reactions to which the predictions were most sensitive. Hence, a conservative approach was taken. In most tests, only a single input parameter was varied. When multiple changes were made, they were generally first made separately and then combined to better evaluate an overall effect.

These tests showed that the mechanism described by the model is highly resilient. There are counterbalancing reactions for many of the species. Often, a change that would appear to be quite significant would not produce a large change in the ozone concentration because a secondary effect of the same change would counterbalance the more obvious outcome.

The basic goal of every change was to fit the experimental results, increase the initial O₃ production rate by approximately a factor of 3 without altering the [T₂]₀ dependency, simultaneously increase the dependence of [O₃]_{SS} on [T₂]₀, and thereby produce much higher [O₃]_{SS} at 1.0% T₂. In addition, the effects of hydrogen addition should be explained.

Over 20 different input parameters and basic assumptions were varied in these tests. Often a range of values was tested for each parameter. To facilitate the discussion, not every test and variation will be presented. Table II lists the major changes and their effect on the initial rate of ozone production and the predicted [O₃]_{SS}. Since most changes were tested at [T₂]₀ = 1.0 and 0.1% the desired

(16) Baulch, D. L.; Cox, R. A.; Hampson, R. F., Jr.; Kerr, J. A.; Troe, J.; Watson, R. T. *J. Phys. Chem. Ref. Data* **1984**, *13*, 1259.

(17) DeMore, W. B.; Molina, M. J.; Watson, R. T.; Golden, D. M.; Hampson, R. F.; Kurylo, M. J.; Howard, C. J.; Ravishankara, A. R. *Chemical Kinetics and Photochemical Data for Use in Stratospheric Modeling*; Evaluation No. 6 and 7, Jet Propulsion Laboratory Publication 83-62 and 85-62; Jet Propulsion Laboratory: Pasadena, CA, 1983, 1985.

(18) H₂O has been shown to accelerate the rate of the hydroperoxyl disproportionation reaction and was treated as a separate reaction in the model. (Kircher, C. C.; Sander, S. P. *J. Phys. Chem.* **1984**, *88*, 2082.)

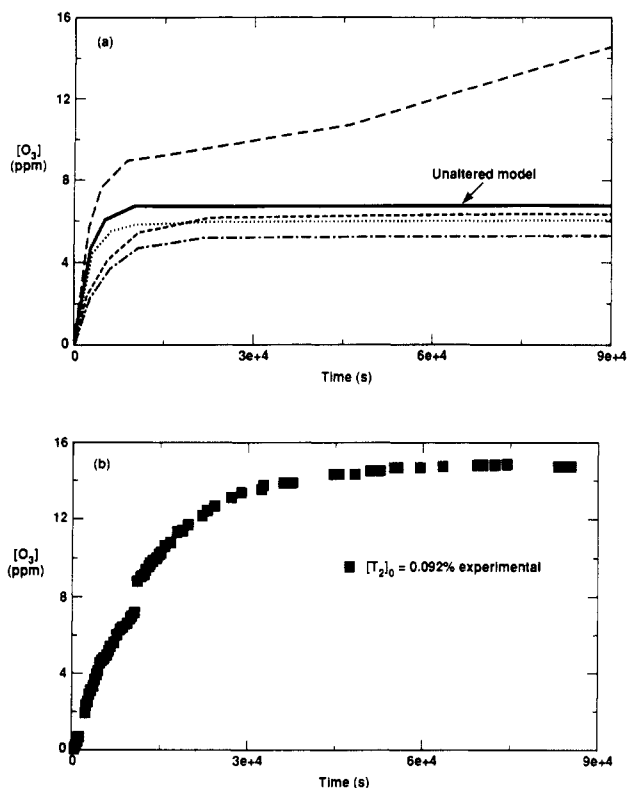


Figure 11. Sensitivity analysis: $[O_3]$ versus time for $[T_2]_0 = 0.1\%$. effects were a large decrease in the initial rate and a large increase in $[O_3]_{SS}$.

Our earlier discussion has shown that

$$[d[O_3]/dt]_{\text{initial}} \propto [T_2]_0 \quad (17)$$

and

$$[O_3]_{SS} \approx \frac{k_7[O]_{SS}}{k_2[TO_2]_{SS}} \quad (22)$$

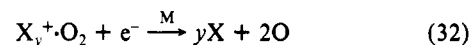
are the equations describing the ozone concentration time dependence. The changes tested were mostly those that altered the main parameters in these equations.

The entries in Table II are grouped by the type of change made. The first category includes changes designed to decrease the predicted initial rate of ozone production (eq 17). To accomplish this, either the radiolytic production of oxygen atoms, the ion-electron recombination production of oxygen atoms, or the rate constant for the ozone formation (eq 7) had to be substantially reduced. A substantial reduction in the rate constant for ozone formation (eq 7) is unreasonable since interest in the depletion of the atmospheric ozone layer has made this rate constant quite well-known,¹⁹ and its uncertainty is far less than the factor of 3 needed to explain the discrepancy in the initial rate prediction and measurement (see Figure 5).

Changes in Oxygen Radiolysis Rates and O Atoms Reactions. Two different changes in the radiolysis of O_2 were tried, a change in the percentage of oxygen atoms produced by radiolysis and a change in overall radiolysis rate. Only when the rate was reduced substantially (beyond the expected uncertainties in the calculation¹⁰) was reduction in the initial rate sufficient to reproduce the experimental results. However, this also resulted in a factor of 3 decrease in $[O_3]_{SS}$ in the 1.0% $[T_2]_0$ case, exactly the opposite of the desired change. All tests that increased the O_2 radiolysis rate produced an increase in both $[O_3]_{SS}$ and the initial rate, which was not the desired effect.

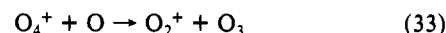
Neither a change in the rate of oxygen atom production from ion-electron recombination, via a change in the reaction rate constants or by forming molecular species as the products, nor an increase in the O atom recombination rate produced a substantial effect.

Changes in Assumptions of Oxygen-Ion Clusters. Next, changes were made to increase the steady-state ozone concentration (see Table II). In earlier reports,¹⁰ the effect of forming oxygen-ion clusters on the model predictions was discussed. In general, these clusters were found to have very little impact on the model. However, if the reaction between ion clusters and electrons resulted in oxygen dissociation



there is a resultant increase in oxygen atom concentration. The fraction of cluster recombinations producing O atoms could be adjusted to produce the desired $[O_3]_{SS}$; however, a different adjustment was needed for each $[T_2]_0$. Formation of O atoms appreciably increased the predicted initial rate of ozone production, rather than the decrease desired.

Very recently we found that the reaction of O_4^+ ($O_2^+ \cdot O_2$) with oxygen atoms is a very fast reaction producing ozone

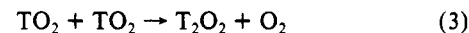


The reaction rate constant was measured to be $(1.8 \pm 1.2) \times 10^{14}$ $\text{cm}^3/(\text{mol}\cdot\text{s})$ ²² though a recent model of solar flares needed to decrease this value to 6×10^{12} $\text{cm}^3/(\text{mol}\cdot\text{s})$ to agree with experimental results.²³

We are unable at this time to test the effects of adding this reaction to the model. However, the addition of this reaction to the model would most likely increase the ozone steady-state concentration and initial production rate. The production of O_2^+ in this reaction would appear to be a source of oxygen atoms via ion-electron recombination (eq 12), thereby increasing the ozone production rate. It must be noted that the measured electron-ion recombination rate constant for O_4^+ is 1 order of magnitude greater than the monomer ion.²⁴ This implies that the concentration of O_4^+ will be very small. Any further modeling of this kind should include O_4^+ formation and all subsequent reactions.

Changes in Hydroperoxyl System Reactions. The next set of changes altered ozone depletion reactions. The major depletion route for O_3 , as shown earlier, is the reaction with hydroperoxyl, eq 2. When the rate constant of this reaction was decreased, a large increase in $[O_3]_{SS}$ was found. However, the relative increase was essentially the same at all $[T_2]_0$ levels and did not alter the 0.3-power dependence on T_2 as was needed to approach the experimental results (compare eqs 24 and 33). This suggests that this rate constant may be part, but not all, of the reason for the model-experiment discrepancies. Only small effects in $[O_3]_{SS}$ resulted from several changes intended to decrease the T atom concentration, and thereby reduce the TO_2 concentration.

The TO_2 concentration was next reduced by increasing the TO_2 disproportionation rate



and resulted in an increase in $[O_3]_{SS}$ but again did not change the 0.3-power dependence on $[T_2]_0$. (We note here that the model includes the work of Kircher and Sander¹⁸ who showed an acceleration of this reaction in the presence of water.)

As discussed earlier, the model predicts that, for the same $[T_2]_0$, $[O_3]_{SS}$ will be reduced by the addition of H_2 . The model predicts that this is due to the removal of O^+ and O_2^+ precursors to ozone and the formation of T atoms, the precursor to TO_2 . Since the model underestimates the reduction in $[O_3]_{SS}$ due to H_2 addition, it is likely that the model is not overestimating the TO_2 depletion effects on ozone. For this reason we do not believe the major

(19) Zerefos, C. S.; Ghazi, A., Eds. *Atmospheric Chemistry, Proceedings of the Quadrennial Ozone Symposium*, Halkidiki, Greece, Sept 1984; Reidel: Boston, 1985.

(20) Huntress, W. J., Jr. *Astrophys. J. Suppl. Ser.* **1977**, *33*, 495.

(21) Adams, N. G.; Smith, D.; Alge, E. *J. Chem. Phys.* **1984**, *81*, 1778.

(22) Fehsenfeld, F. C.; Ferguson, E. E. *Radio Sci.* **1972**, *7*, 113.

(23) Zinn, J.; Sutherland, C. D.; Ganguly, S. *J. Geophys. Res.* **1990**, *95*, 16705.

(24) Dulaney, J. L.; Biondi, M. A.; Johnsen, R. *Phys. Rev. A* **1988**, *37*, 2539.

TABLE III: Methane Reactions Added to the Model To Simulate the Effects of a Limited Amount of Methane as an Impurity in the Gases

reaction	rate constant, cm ³ /(mol·s)	ref
CH ₄ + H ₃ ⁺ → CH ₃ ⁺ + H ₂	1.45 × 10 ¹⁵	20
CH ₄ + H ₂ ⁺ → CH ₃ ⁺ + H ₂ + H	1.4 × 10 ¹⁵	20
CH ₃ ⁺ + e ⁻ → C + 5H	6.6 × 10 ¹⁸	21
CH ₃ ⁺ + e ⁻ → C + 3H	6.6 × 10 ¹⁸	estimate by analogy with CH ₃ ⁺
CH ₄ + O(¹ D) → CH ₃ + OH	8.4 × 10 ¹³	16
CH ₃ + O ₂ → CH ₃ O ₂	2.18 × 10 ¹⁷	16

deficiency of the model is in the hydroperoxyl system.

Impurity Effects. The possibility that impurities in reaction mixture might be important was also considered. To account for the effect of methane on the ozone concentration, several main methane reactions were added to the model. These are listed in Table III. Methane (tritiated or protiated) is a possible impurity in both the tritium and oxygen. The methane content of T₂ gas from the same Pd bed and same 50-cm³ reservoir bottle which were used as the source of T₂ throughout these experiments was 87 ppm. The lot analysis of the cylinder of oxygen used in these experiments gave a methane concentration of <1 ppm. Therefore, in experiments at 1.0% T₂, where the maximum methane concentration would be expected we calculated that the reaction mixture methane concentration would be <2 ppm.

When the CH₄ reactions were included in the model calculations, a large decrease in the initial rate of O₃ production was found. This is due to the reaction of CH₄ with O(¹D) which reduces the oxygen atom concentration. However, the steady-state ozone concentration is essentially unaffected, because once the methane is consumed ozone production proceeds unperturbed. The additional hydrogen atoms formed by electron recombination with CH₃⁺ and CH₂⁺ do not produce sufficient HO₂ to alter the [O₃]_{SS}.

The effect of an unidentified impurity which could react with both oxygen and tritium atoms was considered. This impurity was assumed to react with O and T atoms and to be consumed in the process. This would reduce the initial rate of ozone production by decreasing [O] and would reduce [TO₂⁺] by reducing [T]. We found at low [T₂]₀, [O₃]_{SS} was decreased if large impurity effects were assumed, but for high [T₂]₀, [O₃]_{SS} was relatively unchanged because the impurity was consumed before affecting the overall reaction. We note that a catalyst which is not consumed would potentially have the desired effect.

Walls are well-known to destroy atomic species. A detailed investigation into wall effects was not within the scope of this work. However, removal of oxygen atoms by the walls is not considered likely because comparison of results from experiments using the 10- and 2.5-cm cells show approximately the same initial ozone formation rate in both cells (see Table IV). This is discussed further in the Surface Effects section below.

Addition of Electron Attachment Reactions. Kruger and Olander²⁵ modeled proton radiolysis of oxygen, and included electron attachment reactions which formed O₂⁻ and O₃⁻. As discussed previously,¹⁰ such reactions were not included in our model due to the narrow band of electron energies (near 0.05 eV) where the attachment reactions have significant cross sections.²⁶ Since the cross sections for the ion-electron recombination reactions are quite high at energies above 0.05 eV, it was determined that, for our experimental conditions, the population of low energy electrons would be very small. Therefore, [O₂⁻] would be negligible. Nevertheless, to test this assumption, the electron attachment reactions and subsequent negative ion reactions of Kruger and Olander²⁵ were included in the model. No attempt was made to account for the electron energy distribution expected in the system.

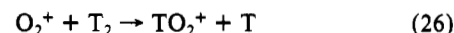
The addition of O₂⁻ and O₃⁻ reactions resulted in a substantial decrease in both the initial rate and [O₃]_{SS}. This is in agreement

TABLE IV: Comparison of 10- and 2.5-cm-Cell Experimental Results

[T ₂] ₀ , %	[O ₃] _{SS} , ppm		initial production rate, ppm/s	
	10 cm	2.5 cm	10 cm	2.5 cm
1.09	49.5 ± 3		1.1 × 10 ⁻²	
0.99	55.0 ± 3		7.2 × 10 ⁻³	
0.93		48.0 ± 3		8.9 × 10 ⁻³
0.10	14.9 ± 0.7		8.8 × 10 ⁻⁴	
0.092	14.8 ± 0.7		1.0 × 10 ⁻³	
0.10		9.1 ± 0.4		8.9 × 10 ⁻⁴
0.11		8.8 ± 0.5		8.9 × 10 ⁻⁴
0.034	7.8 ± 0.4		3.1 × 10 ⁻⁴	
0.028	4.9 ± 0.25		1.5 × 10 ⁻⁴	
0.027	5.3 ± 0.25		1.9 × 10 ⁻⁴	
0.030		3.2 ± 0.5		1.4 × 10 ⁻⁴

with the Elsayed-Ali and Miley²⁷ study of O₃ production by heavy ions. The decrease in the initial rate was very large, and the [O₃]_{SS} was 1 order of magnitude smaller than model predictions in the absence of these reactions. It is very likely that neglecting the details of the electron energy spectrum and its alteration of the ion-electron recombination reactions resulted in too large of a negative ion population, and with a more complete model a smaller decrease in O₃ would be expected. However, this decrease in [O₃]_{SS} is contrary to the experimental measurements.

Effects of Reducing Upper-Limit Rate Constants. For several reactions in the model¹⁰ only upper limit rate constants were available in the literature. Of these reactions, the most important in the ozone cycle is



When the rate constant for this reaction was decreased from the literature upper limit value,²⁰ [O₂⁺] increased and resulted in greater O atom production due to electron-O₂⁺ recombination. A decrease in this rate constant also decreased [TO₂⁺]. The relationship between TO₂⁺ and T₃⁺ via the equilibrium shown in eq 27 was discussed earlier. When the rate constant for the reaction in eq 26 was reduced by factors of 10 and 20, the initial rate of O₃ production increased slightly. The steady-state ozone concentration showed a small increase, mostly at low [T₂]₀.

The O₂⁺ + T₂ reaction must be affected by H₂ addition. In model calculations with added H₂, the reduction of the rate constant for the reaction in eq 26 made a far smaller change in [O₃]_{SS} than was measured in the experiments at 0.1% T₂. Therefore, the upper limit used for this rate constant is apparently not the major source of disagreement between the model and experiment.

From all the tests we have performed, it seems evident that no single change in input parameters can reduce the initial rate of O₃ production and alter the [O₃]_{SS} to match the experimental results. Multiple, specific changes could bring the model into agreement with the experiment, but the correct combination is not clear from these tests.

Surface Effects: Experiment and Model

The steady-state O₃ concentrations and initial rates of O₃ production from experiments in both the 2.5- and 10-cm cells are compared in Table IV and Figure 10. In general, an increase in the surface-to-volume ratio does not change the measured initial rate of O₃ production but does cause a decrease in [O₃]_{SS} for three of the experiments. The surface effects on [O₃]_{SS} are dependent on [T₂]₀, with no detectable reduction at 1.0% T₂, but with obvious reductions in [O₃]_{SS} at 0.1 and 0.03% T₂. The reproducibility of the ozone data in the 2.5-cm cell is evident from Figure 10b.

These results can be explained by assuming limited surface adsorption or depletion of ozone. Surface removal could be sufficiently slow and small that the effect on the initial rate of ozone production would be undetected but would alter steady-state concentrations.

(25) Kruger, V. R.; Olander, D. R. *J. Phys. Chem.* 1976, 80, 1676.

(26) Christophorou, L. G.; McCorkel, D. L.; Anderson, V. E. *J. Phys. B* 1971, 4, 1163.

(27) Elsayed-Ali, H. E.; Miley, G. H. *J. Appl. Phys.* 1986, 60, 1189.

Two approaches were used to test if limited surface removal of O_3 could quantitatively account for the observed differences in $[O_3]_{SS}$ results from the two cells. The first method sought to find a fixed level of ozone absorption per unit surface area, which, when multiplied by the total area and added to the measured $[O_3]_{SS}$, would result in the same total ozone production for a given $[T_2]_0$. However, no fixed level of ozone absorption per unit surface area could be determined which would fit the experimental results. It is possible that with more experimental data a level of adsorption can be found which would fit experimental data.

As a second approach, wall adsorption reactions were added to the gas-phase model itself. It was found that by assuming a limited adsorption of ozone to reduce the predicted initial rate of production and by assuming a significant level of TO_2 adsorption to decrease the ozone destruction reactions, adjustments could be made for each concentration of T_2 which would produce concentrations approaching experimental results. Although a wall effect which changes with $[T_2]_0$ has little physical basis, it does give an indication of which effects should be considered in a more complete, heterogeneous model.

Another effect of decreasing the diameter of the reaction cell is an increased loss of radiolysis energy to the walls. In the gas-phase model, wall losses were not considered. To determine if the wall loss could account for the discrepancies between experiment and model, the fraction of total radiolysis energy absorbed by the walls was calculated. For the 10-cm cell, less than 1% of the total energy was calculated to be lost to the walls, the 2.5-cm-cell loss is calculated to be about 2.5%. Therefore, the energy losses are well within the uncertainty of the radiolysis calculations and cannot account for the measured differences.

It is evident that no explanation presented here completely reconciles the effect of the increased surface-to-volume ratio on the measured O_3 concentration. The closest explanation is a limited adsorption of ozone on the glass.

Conclusions

Experimental results confirmed the presence of ozone as an intermediate in the tritium oxidation reaction. These studies provided the first measurements of an important intermediate of the $T_2 + O_2$ reaction.

The experimental results show a linear increase in the initial rate of ozone production with increasing $[T_2]_0$. As the rate of ozone depletion reactions increase, the ozone concentration reaches a steady state. This is in agreement with predictions of the comprehensive model of the homogeneous reaction.

The experimental data are qualitatively, but not quantitatively reproduced by the model. The measured initial ozone production rate was one-third of that predicted. The steady-state ozone concentration for the $T_2 + O_2$ experiments increased with the 0.6 power of $[T_2]_0$, whereas a 0.3-power dependence was predicted.

The addition of stable hydrogen to the reaction mixture does not affect the initial rate of ozone production, but generally reduces the $[O_3]_{SS}$. A clear correlation between the amount of added H_2 and reduction in $[O_3]_{SS}$ was not found. The effect of the Pyrex surface of the reaction vessel on the ozone concentration varied with $[T_2]_0$, with higher tritium levels being least affected.

Attempts to modify the model by single alteration of a variety of reactions failed to produce agreement with the experimental data. This implies either that a number of the kinetic factors in the model may be significantly in error or that one or more important effects are not contained in the model.

Acknowledgment. We thank Drs. Christopher Gatrousis, Jeffery Richardson, and Carl Poppe for their constant support and encouragement, Prof. Harold S. Johnston for his critical review, and Mr. Terrance Poole and Mr. Stephen Wilson for their excellent mechanical efforts. This work was performed under the auspices of the U.S. Department of Energy by Lawrence Livermore National Laboratory under Contract No. W-7405-ENG-48.

Choice of Gas Kinetic Rate Coefficients in the Vibrational Relaxation of Highly Excited Polyatomic Molecules

György Lendvay[†] and George C. Schatz*

Department of Chemistry, Northwestern University, Evanston, Illinois 60208-3113
(Received: October 24, 1991; In Final Form: January 14, 1992)

We examine the convergence of average energy transfer with maximum impact parameter in classical trajectory studies of CS_2 collisional relaxation by He, Xe, H_2 , CO, CS_2 , and CH_4 , SF_6 relaxation by He, Ar, Xe, and SF_6 , and SiF_4 relaxation by Ar. This leads to estimates of the gas kinetic collision rate coefficient that are substantially larger (by a factor of 3.1 on average, and a maximum of 4.7) than are obtained using the traditional Lennard-Jones collision frequency.

I. Introduction

In unimolecular and chemical activation reactions, vibrational relaxation competes with the chemical reaction. To model such processes one often uses a master equation in which the energy of the reacting molecule is divided into bins,¹⁻⁹ with transitions between bins taking place by energy transfer and loss of population of each bin arising from reaction. Solution of this master equation provides the rate coefficient for the net reactant consumption (the rate of the unimolecular reaction) corresponding to the given temperature and pressure. In this master equation, the rate of the reaction from each energy bin is generally calculated by RRKM theory,¹⁻⁸ while the rate of energy transfer is obtained from a dynamical model for the energy transfer probability distribution $P(E, E')$. This probability is converted to a rate by

multiplying it by the collision rate ω between the reactant and the collision partner at the given pressure and temperature.^{1-6,9}

(1) Robinson, P. J.; Holbrook, K. A. *Unimolecular Reactions*; Wiley: London, 1972.

(2) Forst, W. *Theory of Unimolecular Reactions*; Academic: New York, 1973.

(3) Pritchard, H. O. *Quantum Theory of Unimolecular Reactions*; Cambridge University Press: Cambridge, UK, 1984.

(4) Quack, M.; Troe, J. In *Gas Kinetics and Energy Transfer*; Specialist Periodical Report; The Chemical Society: Burlington House, London, 1977; Vol. 2.

(5) Tardy, D. C.; Rabinovitch, B. S. *Chem. Rev.* 1977, 77, 369.

(6) Gilbert, R. G.; Smith, S. C. *Theory of Unimolecular and Recombination Reactions*; Blackwell: Oxford, UK, 1990.

(7) McCluskey, R. J.; Carr, R. W., Jr. *Int. J. Chem. Kinet.* 1978, 10, 171.

(8) Marcus, R. A. *J. Chem. Phys.* 1952, 20, 359.

(9) Whyte, A. R.; Lim, K. F.; Gilbert, R. G.; Hase, W. L. *Chem. Phys. Lett.* 1988, 152, 377. Lim, K. F.; Gilbert, R. G. *J. Phys. Chem.* 1990, 94, 72.

[†] Present address: Central Research Institute for Chemistry, Hungarian Academy of Sciences, H-1525 Budapest, P.O. Box 17, Hungary.